INTERNATIONAL JOURNAL OF INTEGRATED ENGINEERING
ISSN: 2229-838X e-ISSN: 2600-7916

IJIE

Vol. 16 No. 3 (2024) 15-27
https://publisher.uthm.edu.my/ojs/index.php/ijie

Fabrication and Implementation of PVA Thin Film-based Relative Humidity Sensor

Mohammed Taha Omar Al-haddar[1], Yew-Keong Sin[1]*

[1] *Faculty of Engineering,*
Multimedia University, Persiaran Multimedia, 63100 Cyberjaya, Selangor, MALAYSIA

*Corresponding Author: yksin@mmu.edu.my
DOI: https://doi.org/10.30880/ijie.2024.16.03.002

Article Info

Received: 14 November 2023
Accepted: 3 January 2024
Available online: 29 April 2024

Keywords

PVA, relative humidity sensor, PVA-based sensor, IDE, PCB

Abstract

This paper presents the fabrication of polyvinyl alcohol (PVA)-based relative humidity sensors using copper interdigitated electrodes (IDEs). These sensors were fabricated by patterning copper IDEs onto FR4 fiberglass substrates and coating them with a thin film of PVA. By varying the number of IDE electrode pairs and the concentration of PVA, the sensors exhibited different resistance values, demonstrating an inverse relationship with the number of IDE electrodes and PVA concentration. Additionally, the thickness of the sensing layer, controlled by spin coating speed, affected the resistance of the sensors. The fabricated sensors achieved a humidity measurement range from 50% to 99% RH based on resistance changes. Furthermore, an interface circuit was designed to integrate the fabricated sensors with an ESP8266 microcontroller, achieving accurate measurements above 74% RH.

1. Introduction

Sensors play a crucial role in detecting and measuring various physical properties such as temperature, pressure, humidity, motion, and light, by converting them into electrical signals through transduction techniques. This paper focuses on the measurement of humidity level in the ambient environment and presents a method to fabricate humidity sensors using a thin film of Polyvinyl Alcohol (PVA).

Humidity is an essential parameter with significant implications for weather, climate, human comfort, and health. PVA possesses hydroxyl groups in its structure that can be influenced by the presence of water vapour in the surrounding environment. Hence, PVA was chosen as the sensitive medium for the fabricated humidity sensors. The hydroxyl groups play an important role in the PVA polymer conductivity. Hence, it is possible to implement PVA in the transduction process of humidity by means of its resistivity. There are three objectives in which their execution and discussion are presented throughout this paper. These objectives are:

- To design interdigitated electrodes (IDEs) using printed circuit board (PCB) printing technique.
- To fabricate PVA thin film-based humidity sensor using spin coating method.
- To investigate the effect of varying the number of IDE electrodes, the concentration of PVA and the spin coating speed on the fabricated humidity sensor's resistance.

2. Literature Review

2.1 PVA

The chemical, mechanical, and physical properties of PVA were extensively studied since its initial synthesis by Hermann and Haehnel in 1924 [1]. PVA is described as an odourless, tasteless, and translucent or whitish granular powder, possessing notable characteristics such as thermostability, biodegradability, biocompatibility, and non-

toxicity. It has high solubility in water, partial solubility in ethanol, and insolubility in oils and organic solvents. The semicrystalline structure of PVA is attributed to the presence of hydrogen bonds among its chains, influencing its physicochemical and mechanical properties [2].

The classification of PVA includes fully hydrolysed and partially hydrolysed, which depends on the method of preparation [3]. A fully hydrolysed PVA is obtained through complete hydrolysis of polyvinyl acetate, resulting in a degree of hydrolysis ranging between 98.0% and 99.0%. Partial hydrolysis of polyvinyl acetate leads to a partially hydrolysed PVA with a hydrolysis degree between 84.2% and 89.0%. Additionally, moderately hydrolysed PVA with a commercial degree of hydrolysis ranging from 92.2% to 96.5% can be manufactured [3], [4]. The structural formulas for fully and partially hydrolysed PVA are illustrated in Fig. 1, providing a clear understanding of their molecular structures.

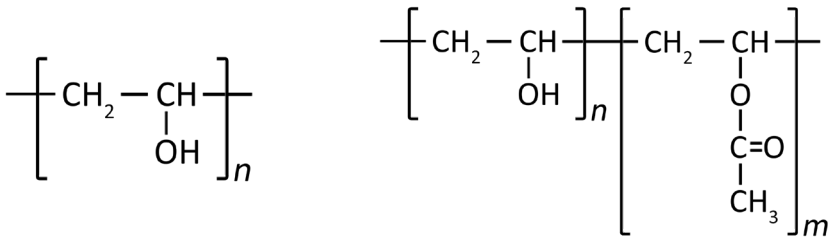

(a) (b)

Fig. 1 *PVA structural formula representation for (a) fully hydrolysed; (b) partially hydrolysed PVA*

2.2 Humidity

Humidity refers to the presence of water vapour in a gaseous atmosphere and can be expressed in various ways. The two most commonly used terms are absolute humidity and relative humidity. Absolute humidity is utilised for primary measurements of water vapour content. On the other hand, relative humidity is utilised for secondary measurements and involves some form of mediation in the measurement of water vapour values. Additionally, there are other types of humidity measurements, such as part per million (PPM) and dew point (T_d), which are subclasses of absolute humidity.

Absolute humidity, also known as vapour density, is defined as the ratio of the mass of water vapour present in a given volume of air. It can be expressed in equation (1) [5].

$$AB = \frac{m_w}{v} \tag{1}$$

Where AB is the absolute humidity measured in g/m^3, m_w is the water vapour mass (g) and v is the volume of air measured in m^3.

Relative humidity is defined as the ratio of the actual moisture content of the air to the maximum amount of moisture that the air can hold at a given temperature and pressure. Since relative humidity is temperature-dependent, it is a relative measurement rather than an absolute value. Relative humidity measurement is expressed as a percentage which can be calculated using the following expression in equation (2) [5].

$$RH = \frac{P_v}{P_s} \times 100\% \tag{2}$$

Where RH is the relative humidity, P_v is the actual partial pressure of moisture content in air (Bar) and P_s is the saturated pressure of moist air (Bar) at the same given temperature.

2.3 Humidity Sensors

Humidity sensors are devices that measure the moisture content of the air. They are utilised in numerous fields, including weather forecasting, industrial process control, building automation, and health and wellness monitoring. Various classifications of humidity sensing instruments have been developed based on different factors. For instance, humidity sensors can be classified based on the type of measurement being taken, such as absolute humidity or relative humidity. Among these, relative humidity sensors are particularly popular due to their low fabrication cost and ease of use in applications related to indoor air quality and human comfort.

Int. Journal of Integrated Engineering Vol. 16 No. 3 (2024) p. 15-27

On the other hand, humidity sensors can be classified based on their sensing element. As discussed by Farahani et al. [5], humidity sensing element can be divided into three main groups. For relative humidity sensors, the sensing element can be a ceramic semiconductor, organic polymer or organic-inorganic hybrid ceramic-polymer. All these three groups translate the change in their electrical and physical properties when absorption or desorption of water vapour occurs into a quantified RH value. Furthermore, Lee and Lee [6] reviewed different types of transduction techniques for humidity sensing. These transduction techniques include optical, gravimetric, capacitive, resistive, piezoresistive and magnetoelastic sensors. Table 1 summarise some of the reported humidity sensors' specifications.

Table 1 *List of humidity sensors with different transduction techniques*

Type	Authors	Humidity Measure.	Materials/ Devices	Sensing Range	Measured output	Ref.
Capacitive	Sun et al.	RH	Ni-doped ZnO nanostructures, Ti/Au IDE	11 – 95%	Capacitance	[9]
	Dwiputra et al.	RH	ZnO Nanorods/WS_2, ITO electrodes	18 – 85%	Capacitance	[10]
	Gu et al.	RH	Polyimide, Al IDE(1)	20 – 70%	Capacitance	[13]
Resistive	Faia et al.	RH	TiO_2 thick film, Ag IDE	10 – 100%	Resistance	[12]
	Leonardi et al.	RH	WS_2 nanosheets, Ag IDE	8 – 85%	Current	[14]
	Chen et al.	RH	WS_2/SnO_2 nanocomposite, Ag IDE	11 – 95%	Current	[15]
	Gupta et al.	RH	Mesoporous ZnO nanosheets (MZNS)	11.3 – 97.3%	Resistance	[16]
Piezo-resistive	Gerlach et al.	RH	Polyimide	10 – 95%	Voltage	[17]
	Buchhold et al.	RH	Polyimide	0 – 100%	Voltage	[18]
Thermal	Okcan et al.	RH	PN-Junction Diode	20 – 90%	Voltage	[19]
	Eigenberg et al.	AB	Negative temperature coefficient (NTC) thermistor	0 – 130 g/m^3	Voltage	[20]
Optical	Kharaz et al.	RH	$CoCl_2$	20 – 80%	Light intensity	[21]
	Schirmer et al.	AB	Spectrometer	1 – 100 ppm	Light intensity	[22]
	Shukla et al.	RH	Nano-like MgO	1 – 85%	Transmitted optical power	[23]
Gravi-metric	Bruno et al.	RH	HMDSO or a-C:H	60 – 100 %	Frequency shift	[24]
Mag-netoelastic	Grimes et al.	RH	Al_2O_3 thin film	2 – 62%	Resonant frequency	[25]

Capacitive humidity sensors have emerged as the dominant type in the market, constituting approximately three-quarters of available humidity sensors [7]. These sensors offer advantages such as low power consumption and strong output signals. They typically consist of conductive interdigitated electrodes (IDEs) patterned on ceramic, glass, or silicon substrates, coated with a hygroscopic sensing layer. Farahani et al. [5] reported that sensing layer can be either a ceramic (metal oxide composite) or a polymeric polyelectrolyte. This is due to their chemical stability, rapid response, and wide temperature range [8]. Sensing performance is influenced by factors like the hygroscopic material's surface-to-volume ratio, as explored by Sun et al. [9] and Dwiputra et al. [10]. The humidity level is determined by measuring changes in the dielectric permittivity of the sensing layer as a result of water molecule absorption or desorption.

Similarly, resistive humidity sensors employ a conductive IDE structure, typically composed of a metallic layer on a glass or ceramic substrate. The IDE structure is coated with a hygroscopic sensing layer, which can be a doped ceramic or an electrolytic conductive polymer [5], [11]. These sensors measure humidity by monitoring changes in the electrical resistance of the sensing medium, which exhibits an inverse exponential relationship with humidity. The adsorption of water vapour leads to dissociation into ionic functional hydroxyl groups, increasing the film's electrical conductivity. This mechanism, first introduced by Theodore von Grotthuss. Furthermore, Faia et al. [12] suggest that various factors, including the number and dimensions of IDE fingers, IDE structure thickness, morphological structure of the sensing medium, surface-to-volume ratio, and sensing layer thickness, impact the resistance value of resistive humidity sensors.

2.4 Grotthuss Mechanism

The Grotthuss mechanism, proposed by Theodor Grotthuss in 1806, is a process governing proton conduction in water and protic solvents [26]. This mechanism plays a crucial role in various chemical reactions in solution, such as acid-base reactions and proton transfer in fuel cells [27]. The protons (H^+ ions) traverse through chains of hydrogen bonds formed by water molecules, known as proton wires, as described by Nagle et al. [28]. The Grotthuss mechanism facilitates rapid diffusion of protons and hydroxide (OH^-) ions through proton transfer between water molecules via hydrogen bonding, leading to the separation of H^+ and OH^- ions through self-ionisation or surface collisions of water molecules [5].

In Grotthuss mechanism, a proton ion hops from one molecule to the next molecule by the exchange of its hydrogen bond with a covalent bond. This leads to the formation of a hydronium ion (H_3O^+) and hydroxide ion (OH^-) as expressed in equation (3) [5], which contribute to the charge transfer in polymer electrolyte membrane (PEM) [27]. In Fig. 2 (a), once a H^+ ion is covalently bounded with a water molecule, it is then followed by tunnelling of this H^+ ion from one water molecule to another. Eventually, this bounded proton is released which leaves the water chain in a polarised state. The net movement of a proton along a single file water chain does not result in the transfer of a unit charge. Therefore, the water chain needs to turn and reorder itself to accept another proton. This water molecules rotation is done through the transport of a Bjerrum D orientation defect [26]. Hence, a unit charge is carried out by the combination of H^+ movement and Bjerrum D defect. Similarly, the transfer of negatively charged hydroxide ion (OH^-), which is called as proton hole, involves two-step process (ion movement and reorientation) as illustrated in Fig. 2 (b). However, the rotation of water molecules is done by the diffusion of a Bjerrum L defect. Both processes, the charge transfer of hydronium ion and proton hole in a PEM, is referred as the protonic conductivity.

$$H_2O + H_2O \leftrightharpoons H_3O^+ + OH^- \tag{3}$$

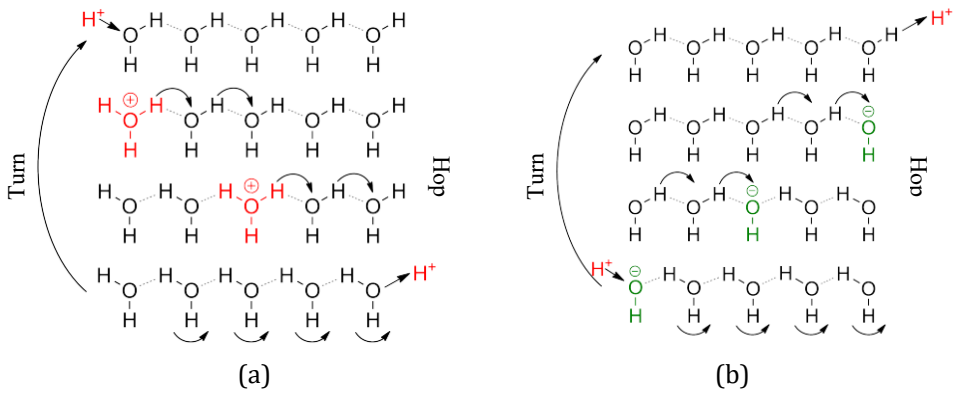

Fig. 2 *Hop and turn Grotthuss mechanism for conductivity of (a) H^+ as hydronium ion along proton wire; (b) OH^- as proton hole along proton wire [26]*

Int. Journal of Integrated Engineering Vol. 16 No. 3 (2024) p. 15-27

2.5 PVA Based Humidity Sensors

The abundance of hydroxyl groups within the PVA structure makes it a suitable material for quantifying water presence in the surrounding environment. Pure PVA or its composites can be used as a hygroscopic sensing medium through different transduction techniques including optical, capacitive and resistive sensors. Table 2 provides different types of relative humidity sensors that utilise PVA in their sensing mechanism.

In optical humidity sensors, the interaction of an optical signal with the gaseous medium at different humidity levels leads to distinct spectrum shifts [29]. Conversely, capacitive and resistive humidity sensors' mechanism is dominated by Grotthuss mechanism. At low humidity levels, the sensor surface exhibits a light coverage of water vapor molecules and dissociated hydroxyl groups. The adsorption and dissociation of water molecules generate free protons (H^+), which facilitate proton hopping between neighbouring hydroxide ion sites (OH^-). As humidity increases, additional water layers form, promoting further dissociation of water molecules and consequently contributing to enhanced protonic conductivity within the sensing layer. This results in a significant change in the sensor's resistance and capacitance.

Table 2 *List of PVA-based humidity sensors with different transduction techniques*

Type	Author	Materials	Measured output	Measured output range	Sensing Range	Ref.
Optical	Somani et al.	PVA/H_3PO_4	Absorbance	-	9 – 100%	[29]
Capacitive	Imawan et al.	PVA-LiCl, Cu/Ag IDE	Capacitance	10pF – 50nF	33 – 94%	[30]
	Rahman et al.	PVA/Graphene flower, IDE	Capacitance	2.35pF – 4.53pF	40 – 90%	[31]
	Rashid H. U.	PVA Nanofiber, Cu IDE	Capacitance	17 pF – 45pF	32 – 92%	[32]
Resistive	Karunarathne et al.	Partially conjugated PVA	Resistance	4.5MΩ – 10.2kΩ	7 – 92%	[33]
	Martadi et al.	PVA, AgAl IDE	Resistance	30.5MΩ – 2.1kΩ	35 – 94%	[34]
	Martadi et al.	PVA/SnO_2 , AgAl IDE	Resistance	22.5MΩ – 27.5kΩ	35 – 94%	[34]
	Rahman et al.	PVA/Graphene flower, IDE	Resistance	7.3MΩ – 0.2MΩ	40 – 90%	[31]
	Deshkulkarni et al.	Polyaniline /PVA Nanocomposite, Cu IDE	Resistance	4.9kΩ – 3.1kΩ	17 – 91%	[35]

3. Humidity Sensor Fabrication

This paper investigates the impact of IDE configuration, mainly the number of fingers, on the resistance of PVA-based humidity sensors. To assess this effect, multiple IDE substrates with varying numbers of finger pairs were fabricated. The first IDE layout consisted of 5 finger pairs, while the second layout featured 8 finger pairs, representing an increase of 3 pairs compared to the first layout. Additionally, a third IDE layout comprised 11 finger pairs. Each gap width, fingers length and the other parameters related to the IDE substrate were kept constant.

The IDE substrates had a width of 20 mm, with their length ranging from 32 mm to 56 mm depending on the number of IDE fingers, as depicted in Fig. 3. The gap between the fingers and the fingers' width were maintained at 1 mm, whereas the distance from the substrate contact pads to the first finger was consistently set at 7 mm across all substrates. The IDE structures were fabricated using a PCB photolithography method in which the layouts in Fig. 3 were used as masks during the patterning process. An industrial flame retardant class 4 (FR4) board, which is a type of fiberglass-reinforced epoxy laminate, coated with 18 µm copper layer was used in the patterning process.

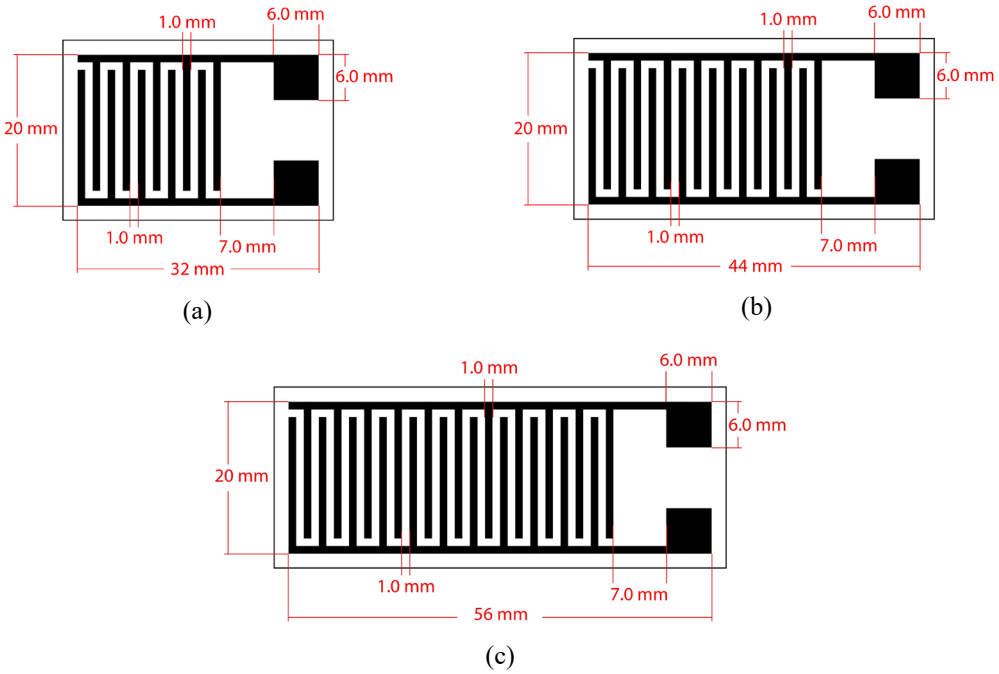

Fig. 3 *Interdigitated electrode layout with (a) 5 finger pairs; (b) 8 finger pairs; (c) 11 finger pairs*

Once the IDE substrates were patterned, PVA polymer was then prepared using a chemically pure partially hydrolysed PVA powder that was produced by Ever Gainful Enterprise Sdn. Bhd. (Petaling Jaya, Malaysia). The PVA was mixed with distilled water without further purification. This PVA has an average molecular weight of 115000 g/mol and a medium dynamic viscosity range between 21.0 to 26.0 mPa-s. In addition, it has a degree of hydrolysis varying between 86 and 89 mol% and a 4% aqueous solution pH of 5.0 - 7.0.

Two different concentrations, 5 wt% and 10 wt% (weight percentage), were prepared to examine the influence of PVA polymer concentration on the resistance of fabricated humidity sensors. The 5 wt% polymer solution was obtained by dissolving 4.99 g of PVA powder in 100 ml of distilled water at 80 °C, while the 10 wt% polymer solution was prepared by dissolving 9.97 g of PVA powder in 100 ml of distilled water at the same temperature. A stirring process was conducted using a hot plate set at 140 °C, ensuring a constant temperature of 80 °C during the mixing procedure. Distilled water was initially heated until the temperature reached 60 °C. Then, the PVA powder was added to the beaker and covered with aluminium foil to prevent water evaporation. The stirring was initiated at a rotation speed of 3 Mot and continued until a clear and transparent polymer solution was obtained. The stirring duration differed for the two polymer concentrations, with the 5 wt% polymer requiring approximately 13 minutes to start turning into a clear mixture, while the 10 wt% polymer took around 42 minutes. The complete dilution of both polymer solutions was achieved after 45 minutes and 120 minutes for the 5 wt% and 10 wt% PVA concentrations, respectively. Subsequently, the mixtures were cooled at room temperature and transferred into tightly closed glass bottles to prevent air exposure.

The two PVA polymers are then deposited onto the IDE substrates using a spin coater. Spin coating is a well-established technique for depositing liquid-like materials onto substrates, with film thickness depending on various factors including its spinning speed. The thickness of the spin-coated layer is typically measured using ellipsometry or surface profilometry. Nevertheless, calculating the layer thickness can be very tedious where multiple models has been proposed such Emslie, Bonner, and Peck and Meyerhofer models. However, these models share a common fact that spin coating thickness is inversely proportional to the square root of coating speed as in equation (4) [36].

$$t \propto \frac{1}{\sqrt{\omega}} \tag{4}$$

Where t is the spin coated layer thickness (nm) and ω is the angular rotation speed (rpm).

By increasing the spinning speed by a factor of two, a 29.3% reduction in the layer thickness can be obtained while increasing the speed by a factor of three leads to a 42.3% reduction in the layer thickness compared to the initial speed layer thickness. Therefore, spin coating speeds of 1000 rpm, 2000 rpm and 3000 rpm were selected for coating the IDE substrates. Prior to spin coating, the IDE substrate contact pads were covered with masking tape since the removal of hardened PVA from the substrate contact pads is very difficult and potentially damage

Int. Journal of Integrated Engineering Vol. 16 No. 3 (2024) p. 15-27

the copper contact pads. Subsequently, the PVA polymer was dispensed onto the IDE substrate using a static dispensing method, with PVA polymer volume of 0.5 ml, 1.0 ml or 1.5 ml depending on the number of IDE finger pairs. After ensuring the substrate was completely covered with the polymer, the spinning process commenced for 10 seconds. The sensors were then placed in an oven at 70 °C for 2 hours. To enable easy and stable measurements, a pair of contact leads were soldered to each sensor's contact pads as shown in Fig. 4. According to Kisiel et al. [37], the joint resistance is estimated to be few milliohms. Therefore, it can be neglected since it will not have a significant effect on the overall sensor resistance.

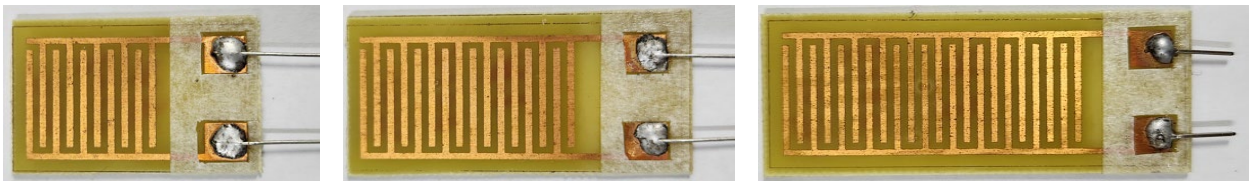

(a) (b) (c)

Fig. 4 *The fabricated humidity sensor with (a) 5 pairs; (b) 8 pairs; (c) 11 pairs of electrodes*

4. Humidity Measurements

Humidity measurement was conducted within a controlled environment using a humidity chamber. The humidity levels inside the chamber were controlled by using dry Nitrogen gas to decrease humidity or a humidifier to increase humidity. The resistance of each fabricated sensor was recorded and in order to evaluate the relationship between their resistance and the IDE electrodes number, PVA polymer concentration and the hygroscopic layer thickness.

4.1 Resistance Measurements

In order to measure the resistance of each sensor, a Keithley 236 Source Measure Unit (SMU) was used. The applied current for the measurement varied depending on the humidity level, ranging from µA to nA. This current adjustment was necessary because when the humidity changes from high to low, i.e., 95% to 65%, the resistance increases from few hundred kilohms to few hundred megaohms. Consequently, a higher voltage drop occurred across the sensor. However, at such high resistance values, the voltage drop exceeded the compliance voltage of the Keithley 236 SMU, making the instrument unable to measure the resistance unless the current was further reduced.

Therefore, a current-voltage (I-V) measurement was executed on the fabricated sensors to verify the linearity of the sensors' resistance measurement. However, the I-V measurements showed that the resistance drastically increases if the current goes bellow 0.0023 µA as shown in Fig. 5. This is due to the applied current is lower than the minimum (threshold) current required for proton hopping to occur. Once the current passes the threshold value, proton hopping elevates the conductivity of the sensor which reduces the sensor's resistance. As a result of the observed limitations, it was determined that the Keithley 236 SMU used in this experiment was not suitable for accurately measuring the resistance of the fabricated sensors.

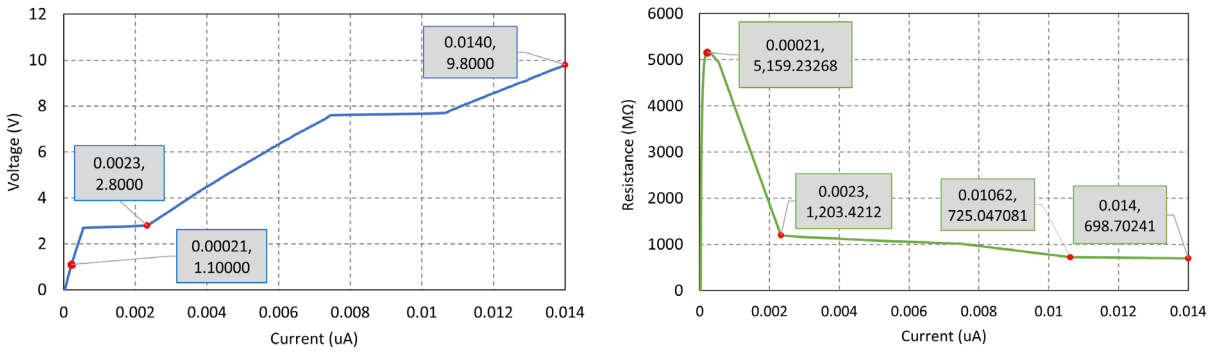

(a) (b)

Fig. 5 *IV measurements interpreted in form of (a) Voltage vs. current; (b) Resistance vs. current*

Furthermore, by constructing a series circuit consist of a digital multimeter with an internal shunt resistor (R_m), a known resistance (R_s), a known DC voltage source (V_s) and the unknown sensor resistance (R_x), it was possible to recalculate the unknown resistance using voltage-division method. The digital multimeter closes the circuit allowing the current to flow through the four components as shown in Fig. 6. Hence, by using equation (5), sensor's resistance (R_x) can be determined based on the voltage reading (V_m) obtained from the digital multimeter.

$$R_x = R_m \left(\frac{V_s}{V_m} - 1 \right) - R_s \tag{5}$$

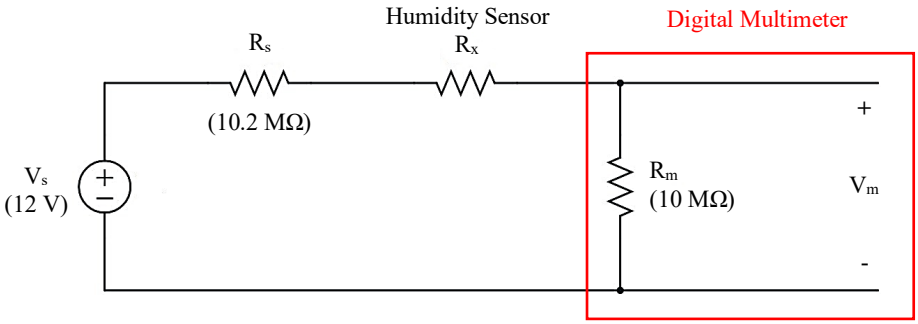

Fig. 6 *Interface circuit used for resistance measurements*

4.2 Measurement Results

The fabricated sensors' resistance was found to have an inverse exponential relationship with the relative humidity. These fabricated sensors showed an average minimum resistance of 0.49 MΩ at 99 %RH, whereas the average maximum resistance reached 1245 MΩ at 50 %RH. However, at humidity below 50 %RH, the voltage reading will be in microvolt (μV) range, which require more advanced measurement tools instead of a digital multimeter to be detected and measured. The fabricated sensors in this project showed higher resistance ratings than the pure PVA-based humidity sensors fabricated by Martadi et al. [34] shown in Table 2. Martadi et al. utilised a 25 mm × 10 mm alumina substrate with IDE fingers and gap width of 0.5 mm for their humidity sensors. Therefore, the variation in resistance profiles can be attributed to the disparities in dimensions between the humidity sensors reported by Martadi et al. and the sensors fabricated in this project.

Generally, the IDE structure provides a large sensing surface area compared to other types of electrodes. This is because of the existence of multiple electrodes on its surface. Fig. 7 (a) shows that each sensor's resistance increases with decreasing the number of electrode pairs on its surface. The sensing mechanism in resistive humidity sensors is related to the conductivity of their hygroscopic medium. Hence, an IDE structure can be visualised as an infinite number of parallel resistors, in which their resistance values are combined and measured through the IDE contact pads. In general, increasing the number of paralleled resistors between two electrodes leads to decreasing the total resistance value between these two electrodes. Therefore, the fabricated sensors with 11 electrode pairs, produce the lowest resistance profile among the other fabricated sensors.

Moreover, the fabricated sensors' resistance was found to vary with the concentration of PVA polymer. Results presented in Fig. 7 (b) reveal that the sensors fabricated with a 10 wt% PVA concentration exhibited a lower resistance response to humidity. This is attributed to the hygroscopic nature of the PVA polymer, which enables it to absorb moisture from the surrounding air. The absorbed water molecules lead to an increase in proton hopping, following the Grotthuss mechanism. As the concentration of PVA polymer increases, its moisture absorption capability also increases, resulting in higher conductivity and subsequently reducing the resistance of the sensors [26], [27], [38].

Int. Journal of Integrated Engineering Vol. 16 No. 3 (2024) p. 15-27

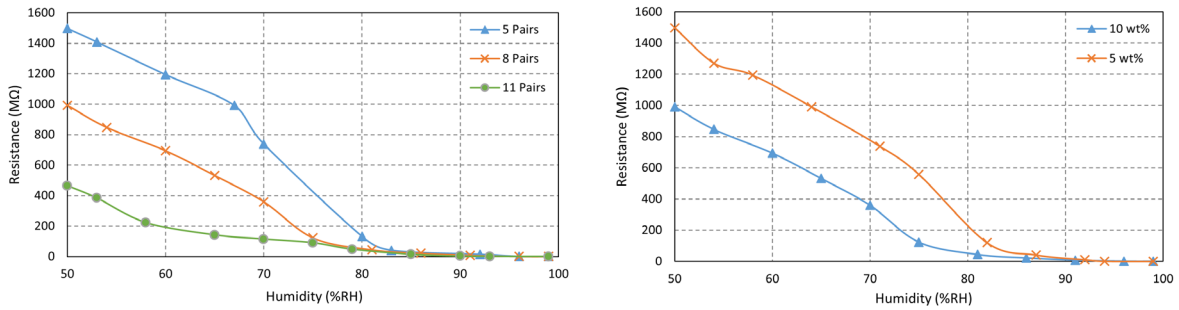

Fig. 7 *Sensor resistance for different (a) IDE electrode pairs; (b) PVA concentration*

Furthermore, the relationship between the sensor's resistance and the spin coating speed was analysed through observations presented in Fig. 8. It was found that sensors fabricated with lower spin coating speeds exhibited reduced resistance profiles. As described in equation (4), the spinning speed is inversely related to the spin-coated sensing layer thickness. In accordance with Adhyapak et al. [39], the study demonstrated that sensors with thicker sensing layers displayed lower resistance. This is due to the increased presence of polymer and hydroxyl groups in thicker PVA sensing layers, allowing for greater absorption of water vapor. Conversely, increasing the spin coating speed resulted in higher resistance values in response to humidity changes.

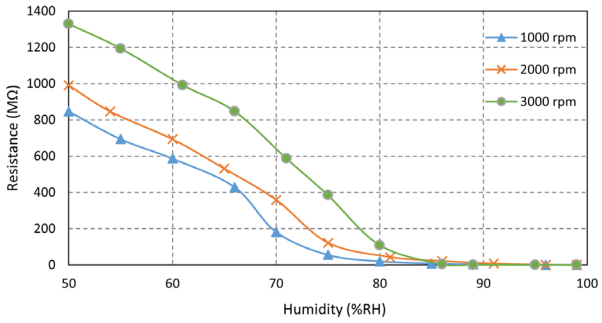

Fig. 8 *Sensor resistance for different spin coating speeds*

5. Sensor Implementation

Since the fabricated humidity sensors have shown an ability to be incorporated into the interface circuit shown in Fig. 6, these sensors can be implemented in real-life applications. Through the use of the collected data and a microcontroller, it was possible to design a prototype that measures humidity level. A microcontroller which has a built-in analog to digital converter (ADC), such as NodeMCU ESP8266, is able to convert analog signals, such as voltage, into digital signals that can be processed by the microcontroller.

NodeMCU ESP8266 has a built-in 10-bit ADC component that allows for 1024 quantisation levels which correspond to a maximum readable voltage of 3.3 V. The ADC component has a shunt resistance (R_{adc}) of 0.32 MΩ. By introducing a 0.34 MΩ resistor as a divider resistor (R_d) into the circuit in Fig. 6, the voltage dropped across R_{adc} at the lowest humidity level (50 %RH) was reduced from 6 V to nearly 3 V. Additionally, the series resistor (R_s) was substituted with a combination of resistors, resulting in the formation of a 0.698 MΩ resistor, which closely approximates the total resistance of R_{adc} and R_d. The prototype circuit diagram and connection configuration are illustrated in Fig. 9 and 10, respectively. Furthermore, due to the modifications made to the interface circuit, the V_m values had to be recalculated using equation (6) based on the measured sensor resistance. Then these V_m values were fed into the source code to enable the microcontroller to translate the resistance into its corresponding humidity level.

$$V_m = V_s \times \frac{R_{adc}}{(R_{adc} + R_d + R_x + R_s)} \quad (6)$$

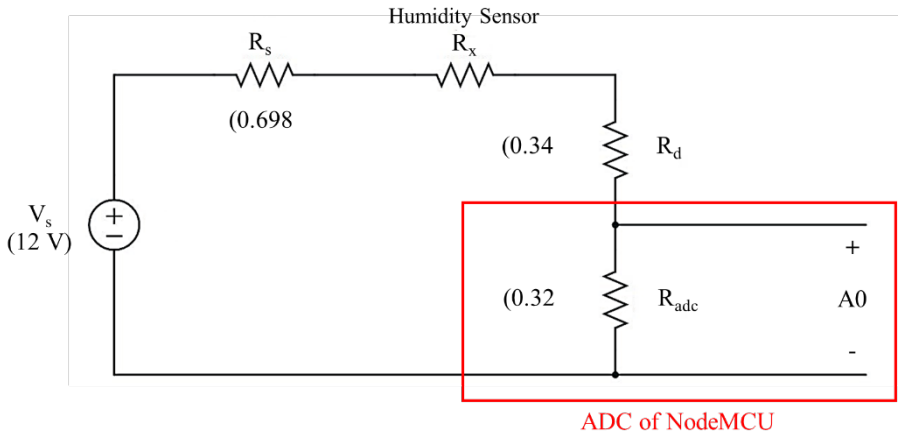

Fig. 9 *Interface circuit diagram of the prototype*

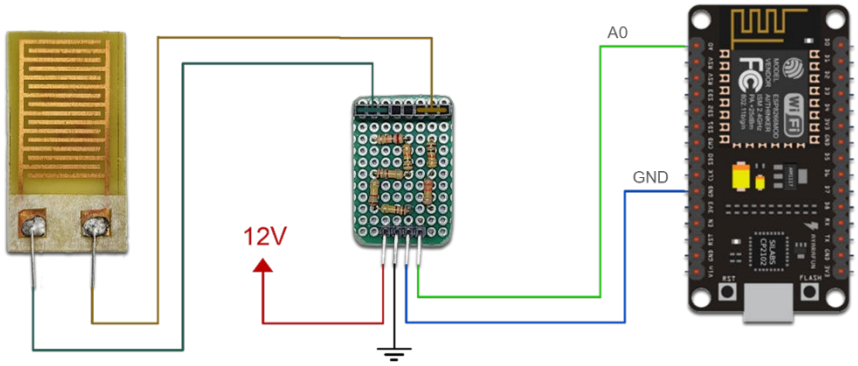

Fig. 10 *Connection configuration of the prototype*

The modified interface circuit shown in Fig. 9 has a maximum and minimum measurable voltage of 6.35 V and 6.28 mV, respectively, and a resolution of 6.269 mV. By comparing the results obtained from equation (6) for all fabricated sensors, it was revealed that the sensors with 11 electrode pairs, 10 wt% PVA polymer concentration, and 2000 rpm spinning speed were found to be suitable for integration with the modified interface circuit. This combination of parameters results in humidity measurement with average step-size between two successive V_m rates equals to 97.21 mV, whereas the step-size voltage goes below the circuit resolution at humidity levels below or equal to 74 %RH. Therefore, when V_m step-size voltage goes below the resolution of the interface circuit, a significant fluctuation was observed in the measured humidity level. This is due to the microcontroller reading being not sufficient to determine the exact voltage corresponding to such low humidity. Fig. 11 demonstrates the final prototype which is based on the circuit configuration in Fig. 10.

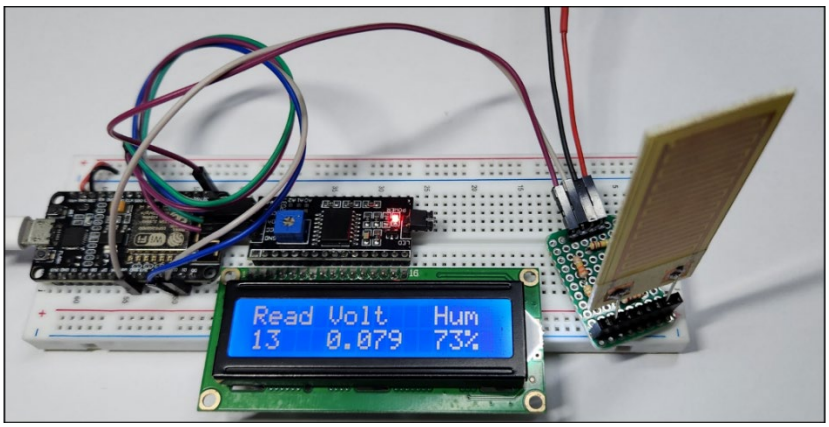

Fig. 11 *Final prototype measuring humidity at 73 %RH*

6. Conclusion

This paper presents a fabrication process of humidity sensors using PCB technique that exhibit sensitivity to ambient water vapor content. The study emphasises the significance of spin coating speed in optimizing the resistance characteristics of humidity sensors, which contributes to advancements in humidity sensing technologies. Furthermore, this research suggests that increasing the number of IDE electrode pairs and PVA polymer concentration reduces sensor resistance. However, due to the high resistance, the fabricated sensors are more suitable for capacitive measurements, as capacitive humidity sensors require a sensing material with low conductivity.

Furthermore, effective implementation between the fabricated sensors and a microcontroller device was demonstrated. This achievement indicates the potential for market integration, that opens an opportunity for subsequent enhancements including sensor size reduction, increased copper layer thickness, and additional IDE finger pairs.

Acknowledgement

The authors would like to express their heartfelt gratitude to Multimedia University for providing the opportunity and support to conduct this research.

Conflict of Interest

The authors would like to declare that there is no conflict of interests regarding the publication of the paper.

Author Contribution

The authors confirm contribution to the paper as follows: ***study conception and design:*** *Mohammed Taha Omar Al-haddar and Yew-Keong Sin;* ***data collection:*** *Mohammed Taha Omar Al-haddar;* ***analysis and interpretation of results:*** *Mohammed Taha Omar Al-haddar;* ***draft manuscript preparation:*** *Mohammed Taha Omar Al-haddar. All authors reviewed the results and approved the final version of the manuscript.*

References

[1] Aslam, M., Kalyar, M. A., & Raza, Z. A. (2018). Polyvinyl alcohol: A review of research status and use of polyvinyl alcohol based nanocomposites. Polymer Engineering & Science, 58(12), 2119–2132.
[2] Abdullah, Z. W., Dong, Y., Davies, I. J., & Barbhuiya, S. (2017). PVA, PVA Blends, and Their Nanocomposites for Biodegradable Packaging Application. Polymer-Plastics Technology and Engineering, 56(12), 1307–1344.
[3] Ben Halima, N. (2016). Poly(vinyl alcohol): review of its promising applications and insights into biodegradation. RSC Advances, 6(46), 39823–39832.
[4] Marin, E., Rojas, J., & Ciro, Y. (2014). African Journal of Pharmacy and Pharmacology Review A review of polyvinyl alcohol derivatives: Promising materials for pharmaceutical and biomedical applications. 8(24), 674–684.
[5] Farahani, H., Wagiran, R., & Hamidon, M. N. (2014). Humidity Sensors Principle, Mechanism, and Fabrication Technologies: A Comprehensive Review. Sensors (Basel, Switzerland), 14(5), 7881–7939.
[6] Lee, C.-Y., & Lee, G.-B. (2005). Humidity Sensors: A Review. Sensor Letters, 3(1), 1–15.
[7] Rittersma, Z. M. (2002). Recent achievements in miniaturised humidity sensors—a review of transduction techniques. Sensors and Actuators A: Physical, 96(2-3), 196–210.
[8] Agarwal, S., & Sharma, G. L. (2002). Humidity sensing properties of (Ba, Sr) TiO_3 thin films grown by hydrothermal–electrochemical method. Sensors and Actuators B: Chemical, 85(3), 205–211.
[9] Sun, N., Ye, Z., Kuang, X., Liu, W., Li, G., Bai, W., & Tang, X. (2018). High sensitivity capacitive humidity sensors based on $Zn_{1-x}Ni_xO$ nanostructures and plausible sensing mechanism. Journal of Materials Science: Materials in Electronics, 30(2), 1724–1738.
[10] Dwiputra, M. A., Fadhila, F., Imawan, C., & Fauzia, V. (2020). The enhanced performance of capacitive-type humidity sensors based on ZnO nanorods/WS_2 nanosheets heterostructure. Sensors and Actuators B: Chemical, 310, 127810.
[11] Roveti, D. K. (2001). Choosing a Humidity Sensor: A Review of Three Technologies. Fierce Electronics. https://www.fierceelectronics.com.
[12] Faia, P. M., Furtado, C. S., & Ferreira, A. J. (2004). Humidity sensing properties of a thick-film titania prepared by a slow spinning process. Sensors and Actuators B: Chemical, 101(1-2), 183–190.
[13] Gu, L., Huang, Q.-A., & Qin, M. (2004). A novel capacitive-type humidity sensor using CMOS fabrication technology. Sensors and Actuators B: Chemical, 99(2-3), 491–498.
[14] Leonardi, S. G., Wlodarski, W., Li, Y., Donato, N., Sofer, Z., Pumera, M., & Neri, G. (2018). A highly sensitive room temperature humidity sensor based on 2D-WS_2 nanosheets. FlatChem, 9, 21–26.

[15] Chen, Y., Pei, Y., Jiang, Z., Shi, Z., Xu, J., Wu, D., Xu, T., Tian, Y., Wang, X., & Li, X. (2018). Humidity sensing properties of the hydrothermally synthesized WS_2-modified SnO_2 hybrid nanocomposite. Applied Surface Science, 447, 325–330.
[16] Gupta, S. P., Pawbake, A. S., Sathe, B. R., Late, D. J., & Walke, P. S. (2019). Superior humidity sensor and photodetector of mesoporous ZnO nanosheets at room temperature. Sensors and Actuators B: Chemical, 293, 83–92.
[17] Gerlach, G., & Sager, K. (1994). A piezoresistive humidity sensor. Sensors and Actuators A: Physical, 43(1-3), 181–184.
[18] Buchhold, R., Nakladal, A., Gerlach, G., & Neumann, P. (1998). Design studies on piezoresistive humidity sensors. Sensors and Actuators B: Chemical, 53(1-2), 1–7.
[19] Okcan, B., & Akin, T. (2004). A thermal conductivity based humidity sensor in a standard CMOS process. 17th IEEE International Conference on Micro Electro Mechanical Systems. Maastricht MEMS 2004 Technical Digest.
[20] Eigenberg, R.A., Nienaber, J.A., Brown-Brandl, T.M. & Hahn, G.L. (2002). Development of rugged environmental monitoring units for humidity and temperature. Applied Engineering in Agriculture, 18(4).
[21] Kharaz, A., & Jones, B. (1995). A Distributed Fibre Optic Sensing System for Humidity Measurement. Measurement and Control, 28(4), 101–103.
[22] Schirmer, B., Venzke, H., Melling, A., Edwards, C. S., Barwood, G. P., Gill, P., Stevens, M., Benyon, R., & Mackrodt, P. (2000). High precision trace humidity measurements with a fibre-coupled diode laser absorption spectrometer at atmospheric pressure. Measurement Science and Technology, 11(4), 382–391.
[23] Shukla, S. K., Parashar, G. K., Mishra, A. P., Misra, P., Yadav, B. C., Shukla, R. K., Bali, L. M., & Dubey, G. C. (2004). Nano-like magnesium oxide films and its significance in optical fiber humidity sensor. Sensors and Actuators B: Chemical, 98(1), 5–11.
[24] Bruno, P., Cicala, G., Corsi, F., Dragone, A., & Losacco, A. M. (2004). High relative humidity range sensor based on polymer-coated STW resonant device. Sensors and Actuators B: Chemical, 100(1-2), 126–130.
[25] Grimes, C. A., & Kouzoudis, D. (2000). Remote query measurement of pressure, fluid-flow velocity, and humidity using magnetoelastic thick-film sensors. Sensors and Actuators A: Physical, 84(3), 205–212.
[26] Miyake, T., & Rolandi, M. (2015). Grotthuss mechanisms: from proton transport in proton wires to bioprotonic devices. Journal of Physics: Condensed Matter, 28(2), 023001.
[27] Yoshida, T., & Tokumasu, T. (2010). Molecular Dynamics Study of Proton Transfer Including Grotthus Mechanism in Polymer Electrolyte Membrane. ECS Transactions, 33(1), 1055–1065.
[28] Nagle, J. F., Mille, M., & Morowitz, H. J. (1980). Theory of hydrogen bonded chains in bioenergetics. 72(7), 3959–3971.
[29] Somani, P. R., & Radhakrishnan, S. (2004). Effect of solid polymer electrolyte on the sensitization of photocurrents in solid-state electrochemical cells using conducting polypyrrole. Journal of Materials Science: Materials in Electronics, 15(2), 75–79.
[30] Imawan, C., Bai, T., & Sri Budiawanti. (2016). A capacitive-type humidity sensor using polymer electrolytes of PVA-LiCl thick films.
[31] Rahman, S. A., Khan, S. A., Rehman, M. M., & Kim, W.-Y. (2022). Highly Sensitive and Stable Humidity Sensor Based on the Bi-Layered PVA/Graphene Flower Composite Film. Nanomaterials, 12(6), 1026.
[32] Rashid, H. U. (2021). Synthesis and Fabrication of Polyvinyl Alcohol Nanofibers Based Capacitive Relative Humidity Sensor. Sir Syed University Research Journal of Engineering & Technology, 11(01).
[33] Karunarathne, T. S. E. F., Wijesinghe, W. P. S. L., Rathuwadu, N. P. W., Karalasingam, A., Manoharan, N., Sameera, S. A. L., Sandaruwan, C., Amaratunga, G. A., & de Silva, S. G. M. (2020). Fabrication and Characterization of Partially Conjugated Poly (Vinyl Alcohol) Based Resistive Humidity Sensor. Sensors and Actuators A: Physical, 314, 112263.
[34] Martadi, S., Sulthoni, M. A., Wiranto, G., Surawijaya, A., & Herminda, I. D. P. (2019). Design and Fabrication of PVA-Based Relative Humidity Sensors Using Thick Film Technology. 2019 International Symposium on Electronics and Smart Devices (ISESD).
[35] Deshkulkarni, B., Viannie, L. R., Ganachari, S. V., Banapurmath, N. R., & Shettar, A. **(**2018). Humidity sensing using polyaniline/polyvinyl alcohol nanocomposite blend. IOP Conference Series: Materials Science and Engineering, 376, 012063.
[36] Spin Coating: Complete Guide to Theory and Techniques. (n.d.). Ossila. https://www.ossila.com.
[37] Kisiel, R., Gasior, W., Moser, Z., Pstruś, J., Bukat, K., & Sitek, J. (2004). $(Sn\text{-}Ag)_{eut}$ + Cu Soldering Materials, Part II: Electrical and Mechanical Studies. Journal of Phase Equilibria & Diffusion, 25(2), 122–124.
[38] Salman, S. A., Bakr, N. A., & Mahmood, M. H. (2014). Preparation and Study of some Electrical Properties of PVA-$Ni(NO_3)_2$ Composites. International Letters of Chemistry, Physics and Astronomy, 40, 36–42.

Int. Journal of Integrated Engineering Vol. 16 No. 3 (2024) p. 15-27

[39] Adhyapak, P., Aiyer, R., Dugasani, S. R., Kim, H.-U., Song, C. K., Vinu, A., Renugopalakrishnan, V., Park, S. H., Kim, T., Lee, H., & Amalnerkar, D. (2018). Thickness-dependent humidity sensing by poly(vinyl alcohol) stabilized Au–Ag and Ag–Au core–shell bimetallic nanomorph resistors. Royal Society Open Science, 5(6), 171986.